

Visible (Red) Vertical-Cavity Surface-Emitting Lasers

G. Tränkle, A. Bhattacharya, A. Oster, J. Sebastian, H. Wenzel, M. Weyers, M. Zorn

Ferdinand-Braun-Institut für Höchstfrequenztechnik
Albert-Einstein-Strasse 11, D-12489 Berlin, Germany
Email: traenkle@fbh-berlin.de Fax: +49-30-6392-2602

Red VCSELs are ideal light sources for emerging technologies such as plastic-fiber-based communication and high-density optical storage systems. However, less favourable materials properties make design and fabrication of AlGaInP-based red VCSELs considerably more challenging than for (In)GaAs/AlGaAs-based near-infrared devices. This paper discusses physics and fabrication of visible VCSELs combining (Al)GaInP-based active regions and AlAs/(Al)GaAs Bragg reflectors, with emphasis on growth by MOVPE of such devices. Details will be discussed at the symposium.

INTRODUCTION

Visible wavelength Vertical Cavity Surface Emitting Lasers (Red VCSELs) are of contemporary interest both at the device research level as well as in the manufacturing environment. The simple change in cavity orientation compared to conventional edge-emitting laser diodes produces radical differences in device design and fabrication, beam characteristics, and scalability [1,2]. The VCSEL's low-divergence, circular output beam makes it a perfect light source for efficient coupling to optical fibers. The very short cavity length ensures that VCSELs operate inherently in a single longitudinal mode. Dynamic-single-frequency operation combined with low threshold currents and high-speed modulation capability make VCSELs ideal for data communications. The ease of forming densely packed two-dimensional arrays, and the possibilities of low cost wafer-scale device production without cleaving, and on-wafer testing and screening are very desirable from the manufacturing standpoint.

The state-of-the-art has progressed rapidly over the last decade and (In)GaAs/AlGaAs-based 850-980nm range VCSELs have moved from the research labs to the marketplace, mainly targeting high-speed, medium-distance data transmission applications like "optobus" links between computer systems and optical interconnects in vehicles and aircrafts [3]. While high-performance 850nm VCSELs are commercially available, heterostructure design for high-performance AlGaInP-based visible-wavelength devices (630-670nm) is, however, considerably more challenging thus making visible VCSELs the focus of intensive research. The development of VCSELs in the visible wavelength region (630-670nm) will be a key enabler for numerous optoelectronic technologies. In particular such red VCSELs would facilitate optical communication systems based on plastic fibers, for which absorption losses are lowest at ~650nm.

CURRENT STATUS OF RED VCSEL RESEARCH

The development of high reflectivity distributed Bragg reflector (DBR) mirrors and the utilization of quantum-well active regions coupled with a variety of different cavity designs have led to a continual improvement in the performance characteristics of VCSELs. Significant milestones in the development include the use of graded interface DBRs to reduce operating voltage and the use of the selective oxidation of AlGaAs to produce efficient current confinement leading to improved power conversion efficiency.

Red VCSELs also have been fabricated with current confinement and index-profiles defined via ion-implantation [4], mesa-formation [5], as well as selective oxidation of AlAs [6,7]; nevertheless the state-of-the-art for AlGaInP-based visible VCSELs is rather modest. For $\lambda \sim 670$ -650nm devices it includes a threshold current of 1.5mA, CW power of 2mW and maximum power conversion efficiency of 10% which have all been demonstrated by the Sandia group [2]. Performance decreases sharply with decreasing wavelength.

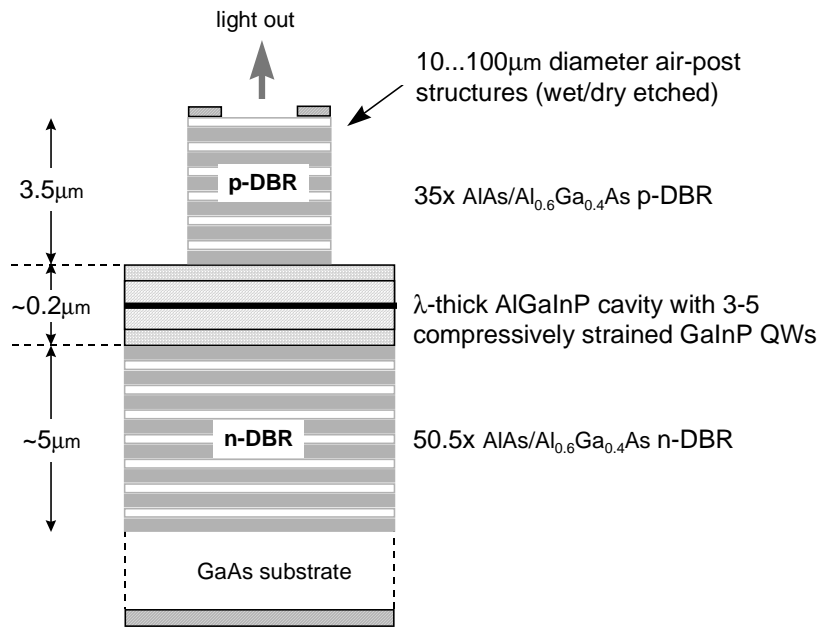


Fig. 1: Schematic structure of a typical visible VCSEL

VISIBLE VCSELS : DESIGN ISSUES

A schematic structure of a typical red VCSEL ($\sim 650\text{nm}$) is shown in Fig. 1. A central optical cavity, usually one wavelength thick, contains compressively-strained GaInP quantum wells embedded within an AlGaInP spacer layer. The cavity is surrounded by quarter-wave $\text{Al}_{0.6}\text{Ga}_{0.4}\text{As}$ / AlAs distributed Bragg reflector (DBR) mirrors to ensure longitudinal confinement of the laser field.

Distributed Bragg Reflectors (DBRs)

At $\lambda \sim 650\text{nm}$ the $\text{Al}_x\text{Ga}_{1-x}\text{As}$ /AlAs DBR mirrors require high Al concentrations ($x \geq 0.5$) in the high-index layer for low absorption. This reduces the index contrast ratio and calls for a large number of DBR periods to achieve the necessary high reflectivities. Since the DBR period at 650nm is about 100nm , the mirror stack for such a VCSEL is $8\text{-}9\mu\text{m}$ thick. The epitaxial growth of such thick layers with extremely stringent demands on the layer thickness and composition is challenging; the paper will present data on the influence of substrate misorientation, growth interrupts and Al-content of the DBR-mirrors on the device performance. Growth on exact-(100) oriented substrates, typically used for Al-GaAs-based edge-emitting lasers, shows a deterioration of mirror quality with increasing number of mirror pairs. This manifests itself as a saturation in the peak reflectivity and can also be correlated to broadening of satellite peaks in the X-ray rocking curve of the superlattices, and an increase in surface roughness. Growths on substrates misoriented 6° towards $\langle 111 \rangle_A$ offer better performance, with the measured reflectivity almost matching the calculated values. This is fortuitous, as the 6° -misoriented substrates are also better suited for the AlGaInP-based active region.

The electrical resistance of the DBR mirrors is another important issue for red VCSEL design. The band offsets between the high- and low-index DBR form potential barriers for charge carriers, which due to the large effective mass of holes are very severe in the p-type DBR. Increased doping levels help decrease resistance, but are accompanied by increased optical absorption losses. The paper will address effective solutions to achieve low-resistance DBR mirrors including the flattening out of barrier spikes at abrupt heterojunctions by the use of alloy grading at interfaces between the DBR layers and including the additional doping at interfaces especially using carbon doping.

Active Region

In VCSELs, the optical cavity is typically one-wavelength thick. The short active region gain medium (typically 20-50nm) results in relatively little gain per pass. Heating of the active region during operation leads to enhanced carrier leakage and further reduced gain. In the case of GaInP/AlGaInP heterojunctions, the situation is further aggravated by the relatively small band offsets in this material system compared to the InGaAs/AlGaAs system. Even GaInP/AlGaInP edge-emitting red lasers suffer from significantly reduced quantum confinement potentials, higher effective masses, poorer thermal conductivities and more temperature sensitive electro-optical characteristics.

For red VCSEL the active region typically consists of 3 to 5 compressively-strained $\text{Ga}_{0.4}\text{In}_{0.6}\text{P}$ quantum wells with lattice-matched $(\text{Al}_{0.5}\text{Ga}_{0.5})\text{In}_{0.5}\text{P}$ or $(\text{Al}_{0.7}\text{Ga}_{0.3})\text{In}_{0.5}\text{P}$ being used for barriers and the cavity. Misoriented substrates, like (100) GaAs tilted 6° towards $\langle 111 \rangle_A$ as used for the growth of the DBR mirrors prevent ordering effects in the AlGaInP and make p-doping easier.

AlGaInP/AlGaAs interfaces

Integrating the AlGaInP-based optical cavity with the AlGaAs-based DBRs is often challenging using low-pressure metal organic vapor phase epitaxy (MOVPE), where AlGaAs and AlGaInP are typically grown at high ($\sim 750^\circ\text{C}$) temperatures. The complete group V switchover required at the DBR/cavity interfaces as well as problems due to In-segregation at the AlGaInP-to-AlGaAs interface can lead to the formation of defects and graded interface layers (Fig. 2a). The problem is further aggravated because the AlGaInP cavity is grown over highly strained thick n:DBR layers. We investigated the influence of the residual strain as well as of various gas flow interrupts and switching sequences at the AlGaInP-AlGaAs-interface. Fig. 2b shows the improvements under optimized conditions.

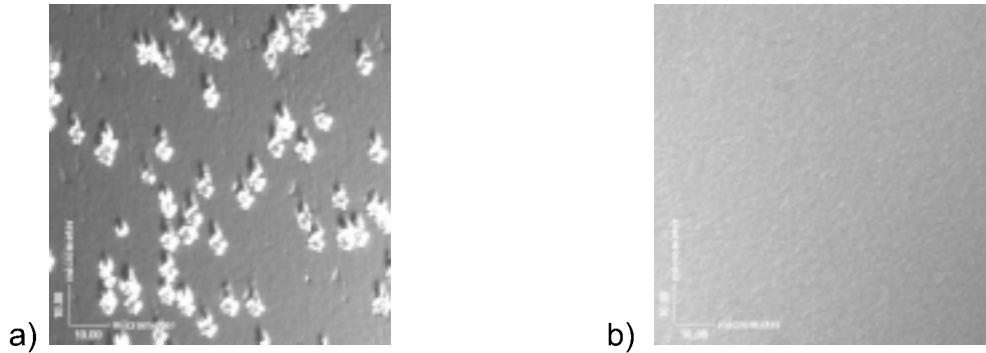


Fig. 2: Dependence of VCSEL surface morphology on gas flow interrupts and switching sequences at the AlGaInP-AlGaAs-interface

DEVICE PERFORMANCE

VCSELs were fabricated by dry-etching air posts with various sizes to achieve transverse optical and electrical confinement. Due to the shift of the cavity resonance along the radius of the wafers devices are available which match the gain curve of the quantum wells of the active region at different wavelength. E.g., Fig. 3 shows the threshold current density of $57\mu\text{m}$ aperture VCSELs measured under pulsed excitation at room-temperature as a function of wavelength. At $\lambda \sim 665\text{nm}$ J_{th} is around $2\text{kA}/\text{cm}^2$, strongly increasing to more than $12\text{kA}/\text{cm}^2$ at 655nm (for QW luminescence $\lambda_{\text{QW}} = 665\text{nm}$). When optimizing the QW design for shorter cavity wavelengths low threshold current densities are achieved at $\lambda \sim 650\text{nm}$. Under pulsed operation the output power of these devices exceeds 5mW .

Doping and grading of the interfaces in the p:DBR mirror also influence threshold current densities. Fig. 4 compares j_{th} as a function of cavity wavelength for different doping and interface schemes in the p:DBR mirror. C-doping of the p:DBR mirror reduces the threshold current densities only slightly compared to Zn-doping. A stronger reduction is obtained when grading the interfaces in the p:DBR mirror. Then threshold current densities below $10\text{kA}/\text{cm}^2$ are obtained even at 643nm . Further reduction in threshold current density is expected by selective oxidation of AlGaAs apertures to confine current flow.

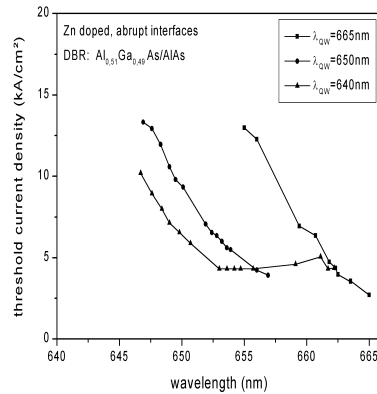


Fig. 3: Room temperature threshold current density of $57\mu\text{m}$ aperture red VCSELs measured under pulsed excitation as a function of cavity and quantum well wavelengths

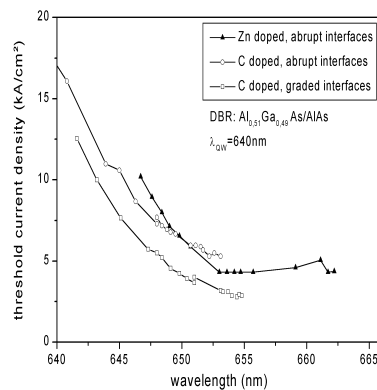


Fig. 4: Room temperature threshold current density of $57\mu\text{m}$ aperture red VCSELs for different doping and interface schemes in the p:DBR mirror

ACKNOWLEDGEMENTS

The authors are grateful for collaborations with F. Bugge, I. Fellner, O. Fink, J. Fricke, S. Gramlich, M. Nasarek, M. Weyers, and U. Zeimer. This project has been supported by the Deutsche Forschungsgemeinschaft and the Alexander-von-Humboldt foundation.

REFERENCES

1. J. L. Jewell, J.P. Harbinson, A. Scherer, Y. H. Lee and L. T. Florez, *IEEE J. Quant. Electron.*, **QE-27** (1991) 1332
2. W. W. Chow, K.D. Choquette, M.H. Crawford, K.L. Lear, and G.R. Hadley, *IEEE J. Quant. Electron.*, **QE-33** (1997) 1810
3. T. Whitaker, *Compound Semiconductor*, **4** (1998) 18
4. R. P. Schneider, K.D. Choquette, J.A. Lott, K.L. Lear, J.J. Figiel, K.J. Malloy, K.M Geib, *IEEE Photon. Tech. Lett.*, **6** (1994) 313
5. R. P. Schneider, M. Hagerott-Crawford, K.D. Choquette, K.L. Lear, S.P. Kilcoyne, J.J. Figiel, *Appl. Phys. Lett.*, **67** (1995) 329
6. J. A. Lott, L.V. Buydens, K.J. Malloy, K. Kobayashi, S. Ishikawa, *Inst. Phys. Conf. Ser.*, **145** (1996) 973
7. K. D. Choquette, R. P. Schneider, M.H. Crawford, K.M. Geib and J.J. Figiel, *Electron. Lett.* **31** (1995) 1145